THE JOURNAL OF BIOLOGICAL CHEMISTRY
Vol. 274, No. 51, Issue of December 17, pp. 36073–36082, 1999

Printed in U.S.A.

Sec-independent Protein Translocation in *Escherichia coli*

A DISTINCT AND PIVOTAL ROLE FOR THE TatB PROTEIN*

(Received for publication, June 30, 1999, and in revised form, September 21, 1999)

Frank Sargent‡§, Nicola R. Stanley‡§¶, Ben C. Berks‡, and Tracy Palmer‡§‖

From the ‡Centre for Metalloprotein Spectroscopy and Biology, School of Biological Sciences, University of East Anglia, Norwich NR4 7TJ, United Kingdom and the §Department of Molecular Microbiology, John Innes Centre, Norwich NR4 7UH, United Kingdom

In *Escherichia coli*, transmembrane translocation of proteins can proceed by a number of routes. A subset of periplasmic proteins are exported via the Tat pathway to which proteins are directed by N-terminal "transfer peptides" bearing the consensus (S/T)RR*X*FLK "twin-arginine" motif. The Tat system involves the integral membrane proteins TatA, TatB, TatC, and TatE. Of these, TatA, TatB, and TatE are homologues of the Hcf106 component of the ΔpH-dependent protein import system of plant thylakoids. Deletion of the *tatB* gene alone is sufficient to block the export of seven endogenous Tat substrates, including hydrogenase-2. Complementation analysis indicates that while TatA and TatE are functionally interchangeable, the TatB protein is functionally distinct. This conclusion is supported by the observation that *Helicobacter pylori tatA* will complement an *E. coli tatA* mutant, but not a *tatB* mutant. Analysis of Tat component stability in various *tat* deletion backgrounds shows that TatC is rapidly degraded in the absence of TatB suggesting that TatC complexes, and is stabilized by, TatB.

In bacteria, transmembrane translocation of proteins can proceed by a number of routes depending upon the nature of both the targeting signal and the substrate. Most proteins destined for export are synthesized with N-terminal extensions, termed "signal peptides," and the translocation event is catalyzed by the general secretory (Sec) apparatus (1, 2). Signal peptides, which direct export via the Sec pathway, show little identity with each other at the amino acid level, although they share similar structures and physicochemical properties (3).

A subset of periplasmic, and periplasmically oriented, proteins are exported via a pathway which operates independently of the core Sec translocon in *Escherichia coli* (4, 5). Substrates of this alternative system are synthesized with, or in some cases associate with partner proteins possessing, N-terminal "transfer peptides" bearing the distinctive (S/T)RR*X*FLK "twin arginine" motif (6). The bacterial twin arginine transfer peptide-dependent protein translocase (Tat system) is apparently both structurally and mechanistically related to the ΔpH-dependent protein import machinery identified in chloroplast thylakoid membranes (7, 8).

Minimally, the Tat machinery comprises four probable membrane proteins: TatA, TatB,[1] TatC, and TatE. The *tatC* gene product is highly hydrophobic and probably contains six transmembrane helices (10). TatA, TatB, and TatE are sequence-related proteins that are predicted to comprise a single N-terminal transmembrane α-helix followed by a water-soluble amphipathic α-helix at the cytoplasmic side of the membrane (11–13). TatA and TatE are more than 50% identical in sequence, while the TatB sequence is more divergent (~25% amino acid identity) and has a considerably extended C-terminal region. The TatA/B/E proteins are homologues of maize Hcf106, the first component of the plant thylakoid ΔpH-dependent pathway to be identified (11).

In-frame deletion mutants of *tatA* or *tatE* exhibit variable, but never complete, defects in the localization of proteins with twin arginine transfer peptides (12). Targeting to the Tat pathway is, however, completely blocked in a Δ*tatA*Δ*tatE* double mutant strain suggesting that TatA and TatE have overlapping essential functions in the Tat system (12).

Two mutant alleles of *tatB* have been described. Weiner and co-workers (9) isolated a point mutant resulting in a leucine for proline substitution at position 22. This *tatB* P22L mutant was unable to correctly localize the twin arginine transfer peptide-dependent trimethylamine *N*-oxide (TMAO)[2] reductase, Me_2SO reductase, or periplasmic nitrate reductase (9). A strain in which *tatB* was disrupted by insertion of a kanamycin resistance cassette has also been described (13). As with the *tatB* P22L mutant, the *tatB*::kan^R insertion mutant was found to be defective in the export of TMAO reductase. However, in marked contrast to a Δ*tatA*Δ*tatE* mutant, the *tatB*::kan^R mutant was reported to be unaffected in membrane targeting and translocation of the transfer peptide-dependent hydrogenase-2, suggesting that TatB is not required for the translocation of all transfer peptide-bearing proteins (13). Furthermore, while TatB is truncated at amino acid 88 in the *tatB*::kan^R mutant, the mutant phenotype of the *tatB* P22L strain can be suppressed by a plasmid encoding only the initial 100 (from a possible 171) amino acid residues of TatB (9). It is therefore conceivable that the N- and C-terminal regions of TatB comprise functionally distinct domains that are differentially affected in the two *tatB* mutant alleles.

In the current work we have sought to define in more detail the roles of the three homologous TatA, TatB, and TatE proteins. An in-frame deletion mutant of *tatB* has been con-

* This research was supported by a Royal Society University Research Fellowship (to T. P.) and Biotechnology and Biological Sciences Research Council Grants B04897 and 88/P09634. The costs of publication of this article were defrayed in part by the payment of page charges. This article must therefore be hereby marked "*advertisement*" in accordance with 18 U.S.C. Section 1734 solely to indicate this fact.

¶ Recipient of Norwich Research Park Studentship.

‖ To whom correspondence should be addressed: Dept. of Molecular Microbiology, John Innes Centre, Norwich NR4 7UH, United Kingdom. Tel.: 44-1603-456-900 (ext. 2726); Fax: 44-1603-454-970; E-mail: tracy.palmer@bbsrc.ac.uk.

[1] Also termed MttA2 (revised nomenclature in GenBank accession number AF067848). Note that this reading frame was incorrectly assigned in the original report (9).

[2] The abbreviations used are: TMAO, trimethylamine *N*-oxide; PCR, polymerase chain reaction; bp, base pair(s); CR, medium of Cohen and Rickenberg.

TABLE I
List of bacterial strains and plasmids featured under "Results and Discussion"

Strain or plasmid	Relevant genotype	Source/reference
E. coli strains		
MC4100	F$^-$, Δ*lacU169,araD139, rpsL150, relA1, pts,F rbsR, flbB5301*	Ref. 14
JARV16	MC4100, Δ*tatA* Δ*tatE*	This work
JARV16-P	JARV16, *pcnB1 zad-981*::Tn*10*d (Kan^R)	This work
BØD	MC4100, Δ*tatB*	This work
BØD-P	BØD, *pcnB1 zad-981*::Tn*10*d (Kan^R)	This work
MCMTA	MC4100, *tatB*::Kan^R	Ref. 13
DADE	MC4100, Δ*tatABCD,* Δ*tatE*	Wexler *et al.* (Footnote 4)
FTD89	MC4100, Δ*hyaB*Δ*hybC*	This work
HD705	MC4100, Δ*hycE*	Ref. 15
Plasmids		
pT7.5	Amp^R	Ref. 16
PFAT65	pT7.5, *tatABCD*	Ref. 12
pFAT217	pT7.5, *tatA*(Δ*B*)*CD*	This work
pFAT222	pT7.5 *tat*(Δ*A*)*BCD*	This work
pFAT228	pT7.5, *tatAB*(Δ*C*)*D*	This work
pNR14	pT7.5, *suflI*$^+$	Stanley *et al.* (Footnote 3)
pNR19	pT7.5, *yacK*$^+$	Stanley *et al.* (Footnote 3)
pBluescript (II KS$^+$)	Amp^R	Stratagene
pFAT415	pBluescript, *tatA*$^+$	This work
pFAT416	pBluescript, *tatB*$^+$	This work
pFAT45	pBluescript, *tatE*$^+$	This work
pFATHP1	pBluescript, *HP0320*$^+$	This work
pFATHP2	pBluescript, *HP1060*$^+$	This work

structed allowing determination of the phenotype of an unambiguously null *tatB* allele, as well as direct phenotypic comparison with previously characterized in-frame deletion mutants in *tatA*, *tatC*, and *tatE* (10, 12). The effects of Δ*tatB* and *tatB*::kan^R mutations on the localization of an extensive range of Tat-dependent substrates have been assessed. Our studies show that TatB is an essential component of the Tat pathway for all the substrates tested. No evidence for phenotypic variation between the two *tatB* alleles was detected. While we confirm a previous report that a portion of hydrogenase-2 activity is associated with the cytoplasmic membrane (13), we go on to demonstrate that this protein is not translocated but remains on the cytoplasmic face of the membrane. Taken together, our results argue against the idea that different Tat components interact with different sets of substrate preproteins. Complementation analysis is used to support the proposal that TatA and TatE are functionally equivalent to one another, but are functionally distinct from the TatB protein. Remarkably, *E. coli* TatA and TatE function can be substituted by TatA from *Helicobacter pylori*, suggesting that only weak amino acid sequence constraints are placed on these essential Tat components. Finally, *in vivo* pulse-chase experiments demonstrate that the TatB protein plays a key role in stabilizing TatC, providing initial evidence for possible complex formation between TatB and TatC.

EXPERIMENTAL PROCEDURES

Bacterial Strains and Growth Conditions—A list of the *E. coli* K-12 strains utilized under "Results and Discussion" of this study are shown in Table I.

During all genetic manipulations, *E. coli* strains were grown aerobically in Luria-Bertani (LB) medium (17). Concentrations of antibiotics were as described previously (12). Growth phenotypes of mutants were determined on M9 minimal medium (17). For all biochemical characterizations, cells were cultured in the medium of Cohen and Rickenberg (CR) (18) fortified as described by Sawers *et al*. (19). For anaerobic respiration, CR was supplemented with glycerol (0.5% w/v) or glucose (0.2% w/v) and TMAO, Me_2SO, sodium nitrate, or sodium fumarate (all at 0.4% w/v) where indicated. For aerobic respiration and anaerobic fermentations, glucose was added to 0.4% (w/v).

Mutant Construction—The *tatB* deletion strain BØD was constructed as follows: a 618-base pair (bp) fragment covering downstream sequence and last eight *tatB* codons was amplified by PCR using primers TATB2 5′-GCGCATCGATCCTTCGTCGAGTGATAAACCGTAA-3′ and TATB3 5′-GCGCGGTACCTTGCGTAAGTCTTCTGGCGAG-3′ with MC4100 chromosomal DNA template. The product was digested with *Cla*I and *Kpn*I and cloned into pBluescript (Stratagene, La Jolla, CA) to give plasmid pFAT163. An 828-bp fragment (upstream sequence and start codon of *tatB*) was amplified using primers TATA1 (12) and TATB1 5′-GCGCGGATCCCACGGATTACACCTGCTCTTTATC-3′ with MC4100 DNA template. The product was digested with *Xba*I and *Bam*HI cloned into pFAT163 to give pFAT164. The *tatB* in-frame deletion allele was excised by digestion with *Xba*I and *Kpn*I and cloned into the polylinker of pMAK705 (20). The mutant allele of *tatB* was transferred to the chromosome of MC4100 as described (20) to give strain BØD.

The *tatA*,*tatE* double deletion strain JARV16 was constructed as follows. A 574-bp fragment covering downstream sequence and final six codons of *tatA* was amplified by PCR using primers TATA6 5′-GCGCATCGATGATAAAGAGCAGGTGTAA-3′ and TATA4 (12) with MC4100 DNA template. The product was digested with *Cla*I and *Kpn*I and cloned into pFAT4 (12) to give plasmid pFAT16. DNA covering the in-frame deletion of *tatA* was excised by digestion with *Xba*I and *Kpn*I and cloned into the polylinker of pMAK705. The mutant allele of *tatA* was transferred to the chromosome of J1M1 (MC4100, Δ*tatE*) (12) to give strain JARV16. Note that JARV16 was constructed as replacement for the original *tatA*,*tatE* double deletion strain, JARV15, described by Sargent *et al*. (12). The strategy adopted for the construction of JARV15 may have inadvertently altered part of a putative *tatB* Shine-Dalgarno sequence located within the *tatA* gene (12). We therefore re-constructed the Δ*tatA*,Δ*tatE* strain maintaining all possible *tatB* Shine-Dalgarno sequences. With respect to Tat-dependent protein export, the JARV16 and JARV15 (12) strains have identical phenotypes (data not shown).

The hydrogenase mutant strain FTD89 was constructed as follows. A 566-bp fragment covering upstream sequence and the first four codons of *hyaB* (encoding the catalytic subunit of hydrogenase-1 (21)) was amplified from MC4100 DNA by PCR using primers HYA1 5′-GCGCTCTAGACATTATCAAAGTACCTGGCTGCCC-3′ and HYA2 5′-GCGCGGATCCCTGAGTGCTCATGCCTGTTTATCC-3′ digested with *Xba*I and *Bam*HI and cloned into pBluescript to give plasmid pFAT420. A 412-bp fragment covering the last five codons and DNA downstream of *hyaB* was amplified from MC4100 chromosomal DNA using the primers HYA3 5′-GCGCGGATCCGTGCAGGTGCGTTAACAGGAAGG-3′ and HYA4 5′-GCGCAAGCTTGCTGTGAATGTCCATTGAGTTGCC-3′, digested with *Bam*HI and *Hin*dIII and cloned into pFAT420 to yield pFAT421. Following digestion with *Xba*I and *Kpn*I, the DNA covering the in-frame deletion of *hyaB* in pFAT421 was transferred to pMAK705 (resulting in plasmid pFAT422), the mutant allele was moved to the chromosome of MC4100 by homologous recombination as described (20) to give strain FTD22 (as MC4100, Δ*hyaB*). A 534-bp fragment covering the upstream DNA sequence and the first three codons of *hybC* (encoding the catalytic subunit of hydrogenase-2 (22)) was amplified from MC4100 DNA using primers HYB1 5′-GCGCTCTAGACGTTCATCATGGGCTTCTCGATTG-3′ and HYB2 5′-GCGCGGA-

TCCCTGGCTCATGCTTTGCTCGCC-3′, digested with *Xba*I and *Bam*HI and cloned into pBluescript to give plasmid pFAT430. A 566-bp DNA fragment covering the last eight codons of *hybC* and downstream sequence was amplified from MC4100 DNA using primers HYB3 5′-GCGCGGATCCGTGGTTTCAGTGAAGGTTCTGTAAT-3′ and HYB4 5′-GCGCAAGCTTCGCTGCCTGTACTTGCGCCTTCGG-3′, digested with *Bam*HI and *Hin*dIII and cloned into pFAT430 to give pFAT431. The in-frame deletion of *hybC* in pFAT431 was excised by digestion with *Xba*I and *Kpn*I, cloned into pMAK705 (resulting in plasmid pFAT432), and transferred to the chromosome of FTD22 as described (20). The resultant Δ*hyaB*,Δ*hybC* strain was named FTD89.

All chromosomal in-frame deletion strains were carefully constructed so to preserve identifiable regulatory elements, coding sequences, stop codons, and Shine-Dalgarno sequences of genes flanking the deletions. Chromosomal deletion strains were confirmed by PCR, and chromosomal PCR products were sequenced to ensure that no point mutations had been introduced.

BØD-P (BØD, *pcnB1 zad-981*::Tn*10*d (Kan^R)) and JARV16-P (JARV16, *pcnB1 zad-981*::Tn*10*d (Kan^R)) were constructed by P1 transduction (23) of the *pcnB1* allele from VJS5833 (kindly provided by Professor V. Stewart). Both *tat* strains were difficult to transduce with P1. Therefore pFAT205, a temperature-sensitive plasmid carrying *tatABCD* (below), was introduced into the *tat* mutants prior to P1 transduction. Transduced strains were selected by virtue of acquired kanamycin resistance, which is linked to the *pcnB* allele. Kanamycin-resistant *tat* mutant strains were subsequently cured of pFAT205 by growth overnight at 44 °C. To confirm the linked *pcnB* allele had been co-transduced into the strains, the yield of plasmid DNA was quantified following transformation of the cured strains with pBluescript and subsequent plasmid purification.

Plasmid Construction—A list of plasmids featured under "Results and Discussion" is shown in Table I. Plasmid pFAT205 carries *tatABCD* in pMAK705. Initially, *tatABCD* was excised from pFAT65 (12) by digestion with *Eco*RI and partial digestion with *Hin*dIII and cloned into pQE60 (Qiagen, Crawley, United Kingdom). The *tat* genes were then excised as a *Xho*I-*Pst*I fragment and cloned into *Sal*I-*Pst*I-digested pMAK705 to give pFAT205.

Plasmid pFAT222, which carries the *tat*(Δ*A*)*BCD* operon with the *tatA* in-frame deletion allele in JARV16, was constructed as follows. A 76-bp fragment covering the start codon of *tatA* and upstream DNA was amplified using primers TATA5 and TATA2 (12) with pFAT65 template. The product was digested with *Eco*RI and *Bam*HI and cloned into the polylinker of pT7.5 (16) to give plasmid pFAT220. A 2236-bp fragment covering the deletion allele of *tatA* to the end of *tatD* was amplified using primers TATA5 and TATD1 with JARV16 DNA template. The product was digested with *Bam*HI and *Xba*I and cloned into pFAT220 to give plasmid pFAT222.

Plasmid pFAT217, which carries the *tatA*(Δ*B*)*CD* operon with the *tatB* in-frame deletion allele of BØD, was constructed as follows. A 350-bp PCR fragment covering the start codon of *tatB* and upstream DNA was amplified using primers TATB1 and TATA5 (12) with pFAT65 template. The product was digested with *Eco*RI and *Bam*HI and cloned into the polylinker of pT7.5 to give plasmid pFAT206. A 2017-bp PCR fragment covering the deletion allele of *tatB* plus *tatC* and *tatD* was amplified using primers TATA5 and TATD1 (12) with BØD chromosomal DNA template. The product was digested with *Bam*HI and *Xba*I and cloned into pFAT206 to give plasmid pFAT217.

Plasmid pFAT228, which carries the *tatAB*(Δ*C*)*D* operon with the in-frame deletion allele of *tatC* present in B1LK0 (10), was constructed as follows. An 840-bp DNA fragment covering *tatA*,*tatB*, and initial three codons of *tatC* was amplified by PCR using primers TATA5 (12) and TATC2 (10) with pFAT65 template. The PCR product was digested with *Eco*RI and *Bam*HI and cloned into pT7.5 to give plasmid pFAT227. A 1760-bp DNA fragment covering the entire *tatAB*(Δ*C*)*D* operon within the chromosome of B1LK0 was amplified by PCR using primers TATA5 and TATA6 (12) with B1LK0 chromosomal DNA template. The product was digested with *Bam*HI and *Xba*I and the released 900-bp fragment cloned into pFAT227 to give plasmid pFAT228.

Plasmid pFAT415 carries the *tatA* gene and more than 500 bp of upstream DNA in pBluescript. It was constructed after PCR amplification of the *tatA* region using primers TATA1 and TATA4 with MC4100 DNA template. Plasmid pFAT416 carries 500 bp of DNA sequence upstream of *tatA* (as in pFAT415) but also the Δ*tatA* allele and the intact *tatB* gene in pBluescript. pFAT416 was constructed by PCR using primers TATA1 and TATA4 and JARV16 DNA template. Plasmid pFAT45 has *tatE* as a 1450-bp insert in pBluescript and was cloned following amplification of the *tatE* region using primers TATE1 and TATE4 (12), with MC4100 chromosomal DNA template. Plasmid pNR42 carries the genes encoding the phage T7 polymerase and the temperature-sensitive λ repressor excised from pGP1-2 (16) and cloned as a 4300-bp *Bam*HI-*Pst*I fragment into the polylinker of pSU18 (24).

In the case of plasmids pFAT23Z (*tatAB*,Δ*C*::*lacZ*,*D*) and pFAT24Z (*tatA*,Δ*B*,Δ*C*::*lacZ*,*D*) the *tatC* gene was replaced from codon 3 to 255 by a complete in-frame *lacZ* coding sequence within the *tat* operon and the (Δ*tatB*) operon as displayed by BØD, respectively. The *lacZ* gene (minus stop codon) was amplified from pAA182 (25) using primers LACZ1A 5′-GCGCCTCGAGATGACCATGATTACGGATTCACT-G-3′ and LACZ2A 5′-GCGCGGGCCCTTTTTGACACCAGACCAACTG-GTA-3′, digested with *Apa*I and *Xho*I and cloned into pBluescript to give plasmid pFAT1Z. DNA covering the final 4 codons of *tatC* and the *tatD* gene was amplified from pFAT65 with primers TATC3Z 5′-GCG-CGGGCCCACTGAAGAATAAATTCAACCGCCCG-3′ and TATD1Z 5′-GCGCGGTACCCGATGGTGAGGCTCGCTCC-3′, digested with *Apa*I and *Kpn*I, and cloned into pFAT1Z to give pFAT1ZD (*lacZ*::*tatC*′*tatD*). DNA covering *tatAB* plus the initial 3 codons of *tatC*, and *tatA*Δ*B* plus the same first 3 codons of *tatC*, was amplified using primers TATA1 (12) and TATC2Z 5′-GCGCCTCGAGTACAGACATGTTTACGGTTTATCA-C-3′ with MC4100 and BϕD DNA template, respectively. PCR products were digested with *Xba*I and *Xho*I and cloned into pFAT1ZD to give plasmids pFAT23Z and pFAT24Z.

Plasmids pFATHP1 and pFATHP2, which carry *H. pylori* 26695 (26) genes *HP0320* and *HP1060,* respectively, were constructed as follows. A 1950-bp region covering *HP0320* and a 600-bp region covering *HP1060* were amplified by PCR utilizing *H. pylori* 26695 chromosomal DNA template. Primers for *HP0320* amplification were HPTA1 5′-GCGCA-TCGATCGAAACCCTATAAAACCTATC-3′ and HPTA2 5′-GCGCGGA-TCCGCTTAATCTCTAGCGGAAATTTTGG-3′, the product was digested with *Cla*I and *Bam*HI and cloned into pBluescript to give pFATHP1. Primers for *HP1060* amplification were HPTBC1, 5′-GCG-CGGATCCGAAAGAAAATTACACTACAATAACG-3′, and HPTBC3, 5′-GCGCTCTAGACCTGTAAATGCGGTTTTAAATCTTC-3′, the product was digested with *Bam*HI and *Xba*I and cloned into pBluescript to yield plasmid pFATHP2. All clones obtained from PCR amplified DNA were sequenced to ensure that no mutations had been introduced.

Protein Methods—Cells were harvested by sedimentation at 7000 × *g* for 15 min at 4 °C, and washed twice in ice-cold 50 mM Tris-HCl (pH 7.6). Periplasmic fractions were prepared by the lysozyme/EDTA method of Osborn *et al*. (27) for 0.5 to 2-liter cultures, or by cold mild osmotic shock for smaller (typically 30 ml) cultures. The method of cold mild osmotic shock involved resuspension of the cell pellet from a 30-ml culture in 7.5 ml of 30 mM Tris-HCl (pH 8.0), 20% (w/v) sucrose, 1 mM EDTA. Following a 10-min incubation at 20 °C, cells were resedimented by centrifugation and the pellet taken up in 2 ml of ice-cold 5 mM $MgSO_4$. After incubation in melting ice for 10 min, the resultant sphaeroplasts were harvested by centrifugation and the supernatant retained as periplasmic fraction. The periplasmic extract was buffered by addition of 100 μl of 1 M Tris-HCl (pH 7.6). Sphaeroplasts were lysed by passage through a French pressure cell and separated into membrane and cytosolic fractions as described (28). Rocket immunoelectrophoresis was performed as described previously (29). Trypsin-catalyzed solubilization of membrane-bound hydrogenase 2 activity from both washed membranes and spheroplasts was performed essentially as described (30, 31). Protein concentration was estimated by the method of Lowry *et al.* (32).

Expression and radiolabeling of *tat* gene products with [^{35}S]methionine (NEN Life Science Products Inc., Boston, MA) from plasmids pFAT65, pFAT217, pFAT222, and pFAT228, under control of the phage T7 ϕ10 promoter, was as described previously (12). Radiolabeled cells were chased by addition of non-radioactive methionine (final concentration 750 μg/ml). Tat substrates preSufI and preYacK from plasmids pNR14[3] and pNR19[3] were expressed under the control of the phage T7 ϕ10 promoter: strains MC4100[pNR42], BØD[pNR42], and MC-MTA[pNR42] were transformed with either pNR14 (pT7.5, *sufI*$^+$) or pNR19 (pT7.5, *yacK*$^+$) and radiolabeling performed as described (12), except 400 μg/ml rifampicin (final concentration) was used. Radiolabeled cells were chased with nonradioactive methionine as above.

Enzyme Assays—β-Galactosidase activity was determined by the method of Miller (23). TMAO and Me_2SO reductase were assayed as the substrate-dependent oxidation of reduced benzyl viologen (33, 34). Acid phosphatase was assayed as the hydrolysis of *p*-nitrophenyl phosphate by the method of Atlung *et al*. (35). Hydrogenase activity in cell fractions was assayed spectrophotomerically as H_2-dependent reduction of

[3] N. R. Stanley, T. Palmer, and B. C. Berks, manuscript in preparation.

oxidized benzyl viologen (28).

In vivo hydrogen oxidation ("uptake") and evolution (formate hydrogenlyase) activities were assayed by a method based on that described by Sawers *et al*. (19) utilizing a "hydrogen electrode," *i.e.* a Clark oxygen electrode adapted for the measurement of hydrogen (Hansatech, Cambridge, United Kingdom). Fumarate-dependent hydrogen uptake was measured as follows. The reaction chamber was filled with 2-ml of 100 mM sodium phosphate (pH 6.8). 25 mM glucose and 2.5 μl of a 50 mg/ml glucose oxidase, 5 mg/ml catalase solution was added to scavenge oxygen. After equilibration for 10 min, 250 μl of hydrogen-saturated 100 mM sodium phosphate (pH 6.8) (equivalent to approximately 203 nmol of molecular hydrogen at 20 °C) was added, followed by a small amount of intact cells (typically 50 μl of a dilute 0.05 g of cells (wet weight) per ml of cell suspension). The reaction was initiated by the addition of 20 mM sodium fumarate. The same protocol was used to measure formate hydrogenlyase activity (formate-dependent hydrogen evolution) although addition of exogenous hydrogen was not required. The reaction was initiated by the addition of 20 mM sodium formate. All enzyme assays were performed in duplicate with results not varying by more than 10% from the mean.

RESULTS AND DISCUSSION

*Phenotype of a Δ*tatB *Mutant Strain*—Previously reported *tatB* mutants would still synthesize TatB protein: either a truncated *tatB* gene product in the case of MCMTA (*tatB*::kan^R) (13) or full-length but amino acid-substituted TatB in the *tatB* P22L mutant (9). As a result it is possible that these mutant strains may retain some TatB functions. We therefore constructed a strain, BØD, in which the *tatB* gene was inactivated by an almost complete in-frame deletion. Using this strain we were able to investigate the phenotypic consequences resulting from a complete absence of TatB protein. In addition, the Δ*tatB* strain allowed direct phenotypic comparison between a *tatB* mutation and the previously characterized in-frame deletion mutants in *tatA*, *tatC*, and *tatE* (10, 12).

We initially assessed the effect of the Δ*tatB* mutation on the localization of two of the Tat pathway substrates studied in earlier characterizations of alternative *tatB* alleles (9, 13). TMAO reductase (TorA) is a water-soluble periplasmic molybdoenzyme that allows *E. coli* to use TMAO as a respiratory electron acceptor (36), and Me_2SO reductase is a complex membrane-bound metalloenzyme required for Me_2SO respiration (37). The Δ*tatB* mutant, BØD, is viable under aerobic respiratory or anaerobic fermentative growth conditions. The strain is, however, unable to grow on the non-fermentable carbon source glycerol with either TMAO or Me_2SO as sole respiratory electron acceptor. Subcellular fractionation studies revealed a complete mislocalization of both TMAO and Me_2SO reductase activities to the cytoplasm in the Δ*tatB* mutant (Table II). These phenotypic effects of the Δ*tatB* mutation are identical to those reported for the *tatB* P22L mutant (9). The *tatB*::kan^R mutant, MCMTA, was also reported to be defective in the translocation of TMAO reductase (13), and we confirm this observation but also demonstrate that Me_2SO reductase is mislocalized in this strain (Table II). Thus, with respect to their effect on TMAO and Me_2SO reductase targeting, the three *tatB* mutant alleles are equivalent.

We next analyzed the effect of the Δ*tatB* and *tatB*::kan^R mutations on the targeting of a further two proteins known to be mislocalized in other *tat* mutants (10, 12). The nitrate-inducible formate:quinone oxidoreductase (formate dehydrogenase-N) is a complex, membrane-bound, metalloenzyme in which the precursor of the active site-containing formate dehydrogenase-N G subunit bears a twin arginine transfer peptide (38). Both subcellular location and enzymatic activity of formate dehydrogenase-N were assessed by rocket immunoelectrophoresis (Fig. 1, *a* and *b*). Formate dehydrogenase-N can be visualized predominantly in the membranes of the parental strain (Fig. 1, *a* and *b, lanes 1* and *5*). However, in both the Δ*tatB* and *tatB*::kan^R mutants membrane targeting of formate dehydrogenase-N is impaired resulting in the cytoplasmic accumulation of catalytically inactive enzyme (Fig. 1, *a* and *b, lanes 2, 3, 6,* and *7*). Hydrogenase 1 is a membrane-bound enzyme in which export of both the peripheral membrane catalytic large subunit and electron transferring small subunit is probably directed by a single twin arginine transfer peptide on the small subunit precursor (39, 40). A third, integral mem-

TABLE II

Localization of enzyme activities in E. coli tat mutants

Oxidoreductase activities are expressed as substrate-dependent benzyl viologen oxidations (units are micromoles of benzyl viologen oxidized per min). Acid phosphatase activities determined as micromoles of *p*-nitrophenyl phosphate hydrolyzed per min. Cells were grown anaerobically on CR medium.

Enzyme	Fraction	Activity (units per g cells)			
		MC4100, parent strain	BØD, Δ*tatB*	MCMTA, *tatB*::Kan^R	DADE, Δ*tatABCD* Δ*tatE*
TMAO reductase[a]	Periplasm	92	<0.01	<0.01	<0.01
	Membrane	<0.01	<0.01	<0.01	<0.01
	Cytoplasm	15	55	45	49
Me_2SO reductase[b]	Periplasm	0.05	<0.01	<0.01	<0.01
	Membrane	2.5	0.06	0.04	0.04
	Cytoplasm	<0.1	1.8	3.5	2.9
Nitrate reductase[c]	Periplasm	0.04	0.07	ND[d]	0.07
	Membrane	33	40	ND	43
	Cytoplasm	2.3	2.8	ND	1.9
Fumarate reductase[e]	Periplasm	<0.01	<0.01	ND	<0.01
	Membrane	2.9	5.1	ND	4.9
	Cytoplasm	0.09	0.17	ND	0.17
Acid phosphatase[f]	Periplasm	0.4	0.4	0.6	0.4

[a] Supplemented with 0.2% glucose and 0.4% TMAO.
[b] Supplemented with 0.2% glucose and 0.4% Me_2SO.
[c] Supplemented with 0.5% glycerol and 0.4% nitrate.
[d] ND, not determined.
[e] Supplemented with 0.5% glycerol and 0.4% fumarate.
[f] Grown aerobically on LB medium. Periplasmic fractions were prepared by cold mild osmotic shock and sphaeroplasts processed further as described under "Experimental Procedures."

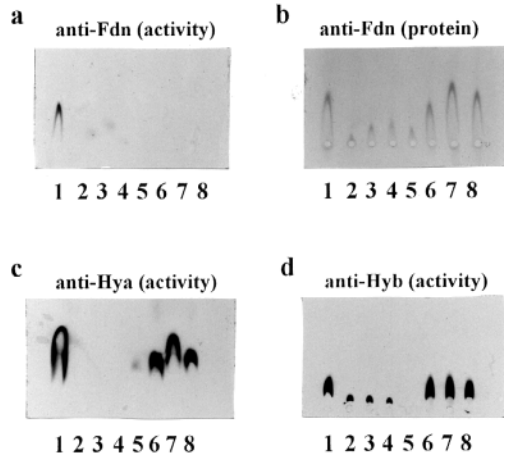

FIG. 1. **Formate dehydrogenase-N and hydrogenases-1 and -2 accumulate in the cytosol in *tatB* mutant strains.** Cells were grown anaerobically with either glycerol plus nitrate to induce expression of formate dehydrogenase-N, or glycerol plus fumarate for maximal expression of the uptake hydrogenases. Sphaeroplasts were formed (lysozyme/EDTA method), further fractionated and rocket immunoelectrophoresis performed as described under "Experimental Procedures." All plates are as follows: *lanes 1*, MC4100 (parental strain), membrane fraction; *lanes 2*, BØD (Δ*tatB*) membrane fraction; *lanes 3*, MCMTA (*tatB*), membrane fraction; *lanes 4*, DADE (Δ*tatABCD,* Δ*tatE*), membrane fraction; *lanes 5*, MC4100 cytosolic fraction; *lanes 6*, BØD, cytosolic fraction; *lane 7*, MCMTA, cytosolic fraction; *lane 8*, DADE, cytosolic fraction. Periplasmic fractions are not shown. All samples represent the same proportion (0.2%) of total protein present in the two fractions. *a,* anti-formate dehydrogenase-N, activity stained; *b,* anti-formate dehydrogenase-N, protein stained; *c,* anti-hydrogenase 1, activity stained; *d,* anti-hydrogenase 2, activity stained.

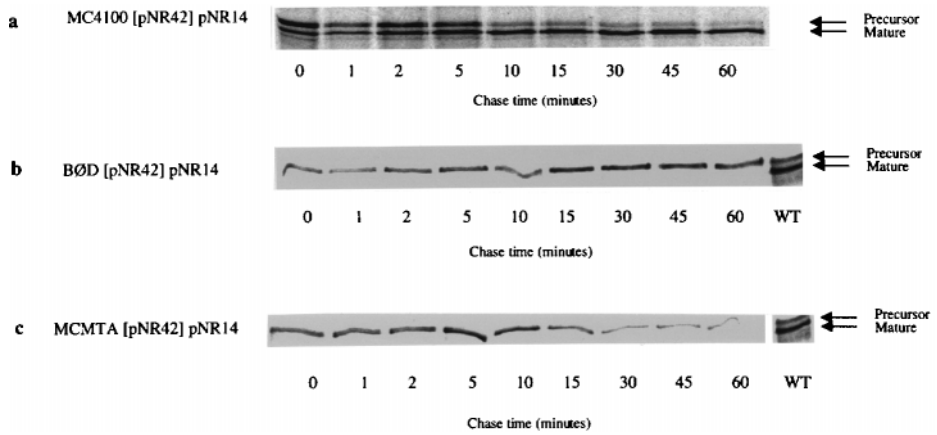

FIG. 2. **Export of SufI is blocked in the *tatB* mutants.** *In vivo* processing of pre-SufI in: (*a*) MC4100, parental strain; *b,* BØD, Δ*tatB;* and *c,* MCMTA, *tatB*::kan^R. In each case precursors were radiolabeled as described under "Experimental Procedures." Samples of whole cells were taken at the time points indicated, proteins separated by SDS-PAGE (12.5% (w/v)) and exposed to photographic film overnight. WT, processing of pre-SufI in MC4100 background after 5-min chase.

brane, subunit is probably also present in the mature enzyme complex (41). Rocket immunoelectrophoresis shows that hydrogenase-1 activity is mislocalized to the cytoplasm in both the Δ*tatB* and *tatB*::kan^R mutants (Fig. 1*c, lanes 2, 3, 6,* and *7*). Thus *tatB* mutations affect hydrogenase-1 targeting but not the insertion of the active site nickel cofactor.

The Δ*tatB* and *tatB*::kan^R mutations were further characterized by assessing the effects of the mutations on the export kinetics of two additional possible Tat pathway substrates, SufI and YacK. Sequence analysis indicates that both these proteins belong to the multicopper oxidase superfamily and are synthesized with twin arginine transfer peptides (6). Yet while YacK is predicted to bind four copper ions per protein monomer, SufI may in fact be devoid of copper cofactors.[3] Pulse-chase analysis of preSufI and preYacK in the parental strain MC4100 shows a time-dependent processing of the precursor proteins into a smaller mature form (Figs. 2*a* and 3*a*). Subcellular fractionation demonstrated that this mature form corresponds to material that has been transported to the periplasmic compartment (data not shown). No processing of either precursor protein was observed when the experiments were repeated in the Δ*tatB* or *tatB*::kan^R mutant backgrounds (Figs. 2, *b* and *c*, 3, *b* and *c*), and subsequent subcellular fractionation confirmed that the radiolabeled precursor proteins remain in the cytoplasm (data not shown). Thus export of SufI and YacK is also completely blocked in the two *tatB* mutants.

The complete mislocalization of all six tested Tat substrates seen in both the Δ*tatB* and *tatB*::kan^R mutants suggests not only that TatB is an essential component of the Tat apparatus but also that the two *tatB* alleles studied are phenotypically equivalent. A complete block in the targeting of TMAO reductase, Me_2SO reductase, formate dehydrogenase-N, and hydrogenase-1 is also exhibited by Δ*tatC* (10) and Δ*tatA*Δ*tatE* strains (12), as well as a strain DADE deleted in all currently known *tat* genes (Table II; Fig. 1, *a*, *b,* and *c, lanes 4* and *8*). Clearly, this is in marked contrast to single Δ*tatA* or Δ*tatE* mutations that only give rise to partial defects in Tat protein localization (12).

Next, we tested the effect of the *tatB* mutations on protein export by the Sec system. Acid phosphatase is one of six phosphatase isoenzymes expressed in *E. coli*, and its targeting to the periplasm is directed by a classic Sec-type leader sequence (42). The acid phosphatase has a pH optimum of 2.5, thus its activity can be easily distinguished from that of the other phosphatases. Moreover, although expressed at a low level aerobically, the expression of the *appA* gene encoding acid phosphatase is maximal in cells growing anaerobically which correlates well with the expression of many of the Tat substrates described in this work (42).

The Δ*tatB* and *tatB*::kan^R mutations had no effect on periplasmic targeting of the Sec-dependent acid phosphatase enzyme (Table II) confirming that TatB is not required for export via the Sec pathway. Furthermore, neither mutation affects the localization of the predominant nitrate reductase and fumarate reductase enzyme activities, both of which are reliant on metallocofactor-binding proteins located at the cytoplasmic face of the membrane (Table II). These observations, together with the cytoplasmic accumulation of some catalytically active Tat substrates, suggest that TatB is not required for metallocofactor insertion.

Export of Hydrogenase-2 Requires a Functional TatB Protein—Hydrogenase-2 is a structurally related isoenzyme of hydrogenase-1 in that the core enzyme comprises a nickel-iron cofactor-binding large subunit and a twin arginine transfer peptide-bearing small subunit (41). Nevertheless, Chanal and co-workers (13) have reported that biosynthesis of this enzyme is unaffected in their *tatB*::kan^R mutant and as a consequence suggested that TatB is not involved in the translocation of all proteins with twin arginine transfer peptides. We have now investigated this observation in more detail. Initially we used rocket immunoelectrophoresis to monitor the subcellular location of the catalytically active peripheral membrane subunits of hydrogenase-2 in various genetic backgrounds. In both the Δ*tatB* and *tatB*::kan^R mutants, while there is considerable mislocalization of hydrogenase-2 activity to the cytoplasm, a small proportion of the activity remains tightly associated with the isolated membrane fractions (Fig. 1*d*). The proportion of membrane-bound hydrogenase-2 activity in the *tatB* mutants was seen to increase in a growth phase-dependent manner, typically reaching 25% of the parental strain in late stationary phase (data not shown). A proportion of hydrogenase-2 activity is also detectable in membranes from a strain deleted in all known *tat* genes (Fig. 1*d, lanes 4* and *8*), and a small amount is present in membranes from Δ*tatC* (40) and Δ*tatA*Δ*tatE* mutants (12). We therefore conclude that, while hydrogenase-2 targeting is severely affected in all the *tat* mutants, a small proportion of hydrogenase-2 activity associates with the membranes in all such strains and not just in the *tatB* mutants.

We next investigated whether the membrane-associated hydrogenase-2 activity detected in the *tat* mutants has been translocated to the periplasmic side of the cytoplasmic membrane. The hydrogenase-2 activities detected by rocket immunoelectrophoresis were assayed using the nonphysiological electron acceptor benzyl viologen (Fig. 1*d*). If the membrane-bound hydrogenase-2 activity represents enzyme that has been correctly translocated to the periplasmic side of the membrane then it might be expected that the enzyme would be able to transfer electrons from hydrogen to its physiological electron acceptor menaquinone. To ascertain whether this was the case we measured whole cell hydrogen oxidation rates with fumar-

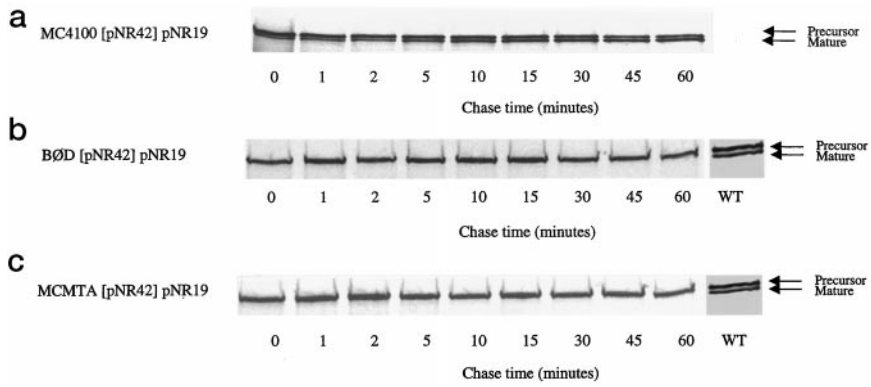

FIG. 3. **Export of YacK is blocked in the *tatB* mutants.** *In vivo* processing of pre-YacK in: *a,* MC4100, parental strain; *b,* BØD, Δ*tatB;* and *c,* MCMTA, *tatB*::kan^R. In each case precursors were radiolabeled as described under "Experimental Procedures," samples of whole cells were taken at the time points indicated, proteins separated by SDS-PAGE (12.5% (w/v)) and exposed to photographic film overnight. WT, processing of pre-Yack in MC4100 background after 5-min chase.

ate as electron acceptor. In these experiments the menaquinone reduced to menaquinol by hydrogenases-1 and -2 is reoxidized via fumarate reductase, an enzyme that does not require the Tat system for biosynthesis (Table II). Fumarate-dependent hydrogen uptake was found to be completely abolished in the Δ*tatB* and *tatB*::kan^R mutants, as well as in the complete *tat* deletion mutant (DADE) and in a control strain (FTD89) which has in-frame deletions in the genes coding for the catalytic subunits of both hydrogenases-1 and -2 (Table III). During fermentative growth *E. coli* synthesizes a third hydrogenase isoenzyme (hydrogenase-3) as part of the cytoplasmically oriented formate hydrogenlyase complex in which electrons derived from formate oxidation are used to reduce protons to hydrogen (41). Control experiments show that *tat* mutations have no effect on hydrogen evolution by this cytoplasmically located hydrogenase indicating that Hyc biosynthesis is Tat-independent (Table III).

Clearly the membrane-localized hydrogenase-2 activity in the *tat* mutants is not physiologically active. This would be consistent with a defect in the export of the benzyl viologen-reactive peripheral membrane subunits, but could also conceivably be caused by inactivity of electron transfer components located between the core hydrogenase and the menaquinone pool. In order to distinguish between these two possibilities we attempted to determine directly whether any of the membrane-associated hydrogenase-2 was located on the periplasmic side of the cytoplasmic membrane. In the parental strain, the peripheral membrane subunits of hydrogenase-2 are anchored to the periplasmic face of the plasma membrane by a short hydrophobic domain at the extreme C terminus of the small subunit (31). Limited trypsinolysis results in specific proteolytic cleavage of the C-terminal domain of the small subunit at its exposed N-region. As a result, the peripheral membrane subunits are released as a stable, water-soluble fragment that retains catalytic activity with benzyl viologen as electron acceptor (30, 31, 43). Trypsin treatment of sphaeroplasts formed from the parental strain MC4100 resulted in the release of benzyl viologen-linked hydrogenase activity into the sample medium over time (Fig. 4*a*, ♦). No hydrogenase release from these sphaeroplasts could be detected in the absence of protease (Fig. 4*b*, ♦). In contrast, only a small amount of hydrogenase activity could be detected in the trypsin-treated soluble protein fractions of sphaeroplasts prepared from the Δ*tatB* and *tatB*::kan^R mutants (Fig. 4*a*, ■ and Δ). Furthermore, the levels of soluble hydrogenase activities released from the *tatB* mutant sphaeroplasts were almost identical to those measured in the control experiment in the absence of trypsin (Fig. 4, *b*, ■, and *b*, Δ). Thus the small amount of hydrogenase release detected was due to leakage from the cytoplasm of the soluble, active hydrogenase precursors identified in the *tatB* mutants (Fig. 1, *a* and *b*) as opposed to enzyme-catalyzed release. It was, however, possible to release the membranous hydrogenase-2 activity found in the *tatB* mutants by trypsin treating isolated membranes rather than sphaeroplasts (data not shown). Taken together, these data demonstrate that hydrogenase-2 is not translocated in the *tatB* mutants. However, a proportion of the active cytoplasmic precursor binds to the cytoplasmic face of the plasma membrane probably, given the trypsin sensitivity of this material, via the same hydrophobic C-terminal domain that would normally anchor these subunits to the periplasmic face of the membrane.

TABLE III
Hydrogen metabolism in tat strains

Strains to be analyzed were grown anaerobically in CR media with either 0.5% glycerol and 0.4% fumarate for hydrogen uptake determination, or fermentatively in 0.4% glucose for hydrogen evolution experiments. Hydrogen uptake and evolution were determined in intact cells with a hydrogen sensing electrode, as described under "Experimental Procedures."

Strain	Hydrogen uptake[a]	Hydrogen evolution[b]
	μmol H_2 oxidized/min/g cells	*μmol H_2 produced/min/g cells*
MC4100	14	15
BØD (Δ*tatB*)	<0.01	23
MCMTA (*tatB*::Kan^R)	<0.01	25
DADE (Δ*tatABCD,* Δ*tatE*)	<0.01	25
FTD89 (Δ*hyaB,* Δ*hybC*)	<0.01	19
HD705 (Δ*hycE*)	20	<0.01

[a] Measured as fumarate-dependent hydrogen uptake.
[b] Determined as formate-dependent hydrogen evolution (formate hydrogenlyase).

It is notable that, in contrast to hydrogenase-2, the closely related *E. coli* hydrogenase-1 isoenzyme displays no membrane association in the *tat* mutant strains even though all enzymes of this type have weakly homologous membrane anchor regions at the C terminus of the small subunit (44). In the case of integral membrane proteins, the orientation of transmembrane regions is normally fixed by the distribution of basic amino acids close to the transmembrane helix ends according to the "positive-inside rule" (45). In the absence of an active translocation system, it is therefore conceivable that the hydrogenase-2 small subunit possesses sufficient basic residues within the N-region of the C-terminal anchor domain (including those that are the target for trypsin proteolysis) such that this transmembrane helix region can insert into the membrane at low efficiency, either in an inverted orientation or as a helical hairpin. In contrast, hydrogenase-1 lacks basic residues in this region. Furthermore, the ability of small subunits to maintain hydrogenase attachment at the periplasmic face of the membrane in mutants devoid of a third, hydrogenase-specific, integral membrane subunit varies between enzymes from different biological systems (46, 47), indicative of variable membrane affinities between related proteins. The reason for this variable behavior is unclear but may also underlie the differing behavior of *E. coli* hydrogenases-1 and -2 in *tat* mutants.

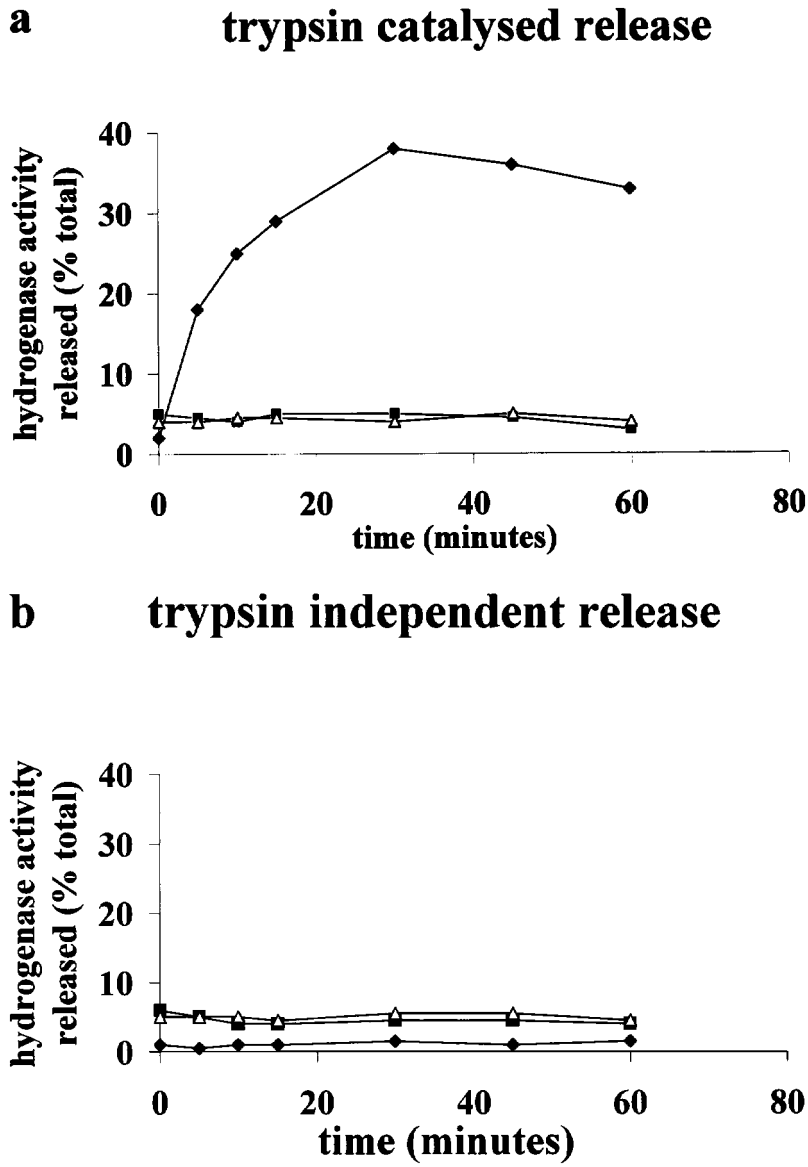

FIG. 4. **Hydrogenase 2 is not translocated in the *tatB* mutants.** Cells were harvested in stationary phase and sphaeroplasts formed by the lysozyme/EDTA method described under "Experimental Procedures." Sphaeroplasts were incubated with: *a,* 0.25% (w/v) trypsin; or *b,* without trypsin, and soluble hydrogen: benzyl viologen oxidoreductase activities measured at the time points indicated. Hydrogenase activity was released from: (♦) MC4100, parental strain; ■, BØD, Δ*tatB*, and Δ, MCMTA, *tatB*::kan^R derived spheroplasts. Enzyme activities are expressed relative to the total cellular hydrogenase activities determined after disruption of sphaeroplasts.

Transcomplementation Analyses of tatB Mutants—With a well characterized Δ*tatB* allele in hand we were able to examine the functional interrelationships between the homologous TatA, TatB, and TatE proteins by means of complementation analysis. In these experiments the *tat* genes under test were carried on a plasmid and expressed under the control of the *tatA* promoter. Complementation was assessed as the ability of the tested genes to restore periplasmically located TMAO reductase activity (*i.e.* a TorA$^+$ phenotype) to the mutant strains.

The TorA$^-$ phenotype of all mutant strains tested (Δ*tatA*Δ*tatE*, Δ*tatB*, *tatB*::kan^R, and Δ*tatABC*Δ*tatE*) could be suppressed by pBR322-based plasmids harboring the entire *tatABCD* operon (data not shown). However, we found it impossible to complement the Δ*tatB* and *tatB*::kan^R mutants *in trans* with high (pBluescript) or moderate (pSU18) copy number plasmids expressing the *tatB* gene alone (data not shown). Indeed, such plasmids even rendered the parental strain MC4100 TorA$^-$ suggesting that increasing the cellular levels of TatB relative to the other Tat proteins prevents the Tat system from functioning. In an attempt to circumvent this stoichiometry problem we introduced the *pcnB1* mutation, an allele that restricts the copy number of ColE1-type plasmids such as pBluescript (48), into the Δ*tatB* strain BØD by P1 transduction resulting in the strain BØD-P. The *pcnB1* allele was also introduced to the Δ*tatA*Δ*tatE* mutant JARV16 to yield the strain JARV16-P, although it should be noted that this was not strictly necessary for successful plasmid complementation of this strain (data not shown).

In the presence of the *pcnB1* mutation the block on TorA export in a Δ*tatB* strain can now be corrected by the provision of *tatB in trans* (Table IV) but not by additional plasmid-borne copies of either the *tatA* or *tatE* genes (Table IV). The TorA export defect in JARV16-P (Δ*tatA*Δ*tatE, pcnB1*) can be fully corrected by supplying only one of the *tatA* or the *tatE* genes *in trans*, but not by providing the cells with extra copies of *tatB* on a plasmid (Table IV). These results support the idea that the TatA and TatE proteins are functionally interchangeable, but that the role of the homologous TatB protein in Tat-dependent export is distinct from that of TatA and TatE. Moreover, the data presented earlier in this work demonstrate that this functional division does not correspond to interactions with two different pools of precursor proteins.

TatB Stabilizes the tatC Gene Product—It is likely that at least some of the known *tat* gene products interact directly with each other and may even form complexes. We considered it feasible that the loss of such interactions in single *tat* gene mutants might manifest itself as a decrease in the stability of the Tat proteins that normally interact with the missing

TABLE IV

Periplasmic TMAO reductase activity in complemented tat strains

Strains were grown anaerobically in CR media with 0.2% glucose and 0.4% TMAO. Periplasmic fractions were isolated by cold mild osmotic shock as described under "Experimental Procedures."

Strain	Specific activity
	μmol/min/mg protein
MC4100	3.45
BØD-P (ΔtatB, pcnB1)	<0.01
BØD-P pFAT415 (Δ*tatB, pcnB1* + p*tatA*)	<0.01
BØD-P pFAT416 (Δ*tatB, pcnB1* + p*tatB*)	2.4
BØD-P pFAT45 (Δ*tatB, pcnB1* + p*tatE*)	<0.01
BØD-P pFATHP1 (Δ*tatB, pcnB1* + p*HP0320*)	<0.01
BØD-P pFATHP2 (Δ*tatB, pcnB1* + p*HP1060*)	<0.01
JARV16-P (Δ*tatA,* Δ*tatE, pcnB1*)	<0.01
JARV16-P pFAT415 (Δ*tatA,* Δ*tatE, pcnB1* + p*tatA*)	2.9
JARV16-P pFAT416 (Δ*tatA,* Δ*tatE, pcnB1* + p*tatB*)	<0.01
JARV16-P pFAT45 (Δ*tatA,* Δ*tatE, pcnB1* + p*tatE*)	2.3
JARV16-P pFATHP1 (Δ*tatA,* Δ*tatE, pcnB1* + p*HP0320*)	0.45
JARV16-P pFATHP2 (Δ*tatA,* Δ*tatE, pcnB1* + p*HP1060*)	<0.01

gene product.

In order to assess the relative stabilities of the *tat* gene products, the plasmid pFAT65, harboring the *tatABCD* operon under the control of an inducible T7 promoter, was introduced into the Δ*tatABCD*Δ*tatE* strain DADE. Following induction of plasmid-borne *tat* gene expression the cells were labeled with [^{35}S]methionine for 5 min followed by a 60-min chase with excess non-radioactive methionine. No significant degradation of the *tat* gene products was observed (Fig. 5, *a, b,* and *c*). Note that by a similar approach we have been able to establish that the radiolabeled Tat proteins produced by pFAT65 are targeted to their predicted cellular compartments (membrane for TatA, -B, and -C, and cytoplasm for TatD).[4] This suggests that a functional Tat apparatus would be produced in these experiments and pFAT65 can indeed suppress the mutant phenotype of the Δ*tatABCD*Δ*tatE* strain (data not shown).

The *tatB* deletion found on the chromosome of BØD was introduced into pFAT65 producing the *tatA*(Δ*B*)*CD* plasmid pFAT217. Pulse-chase analysis using this plasmid in the Δ*tatABCD*Δ*tatE* strain, DADE, allows an estimate of the relative stabilities of the *tat* operon products in a *tatB* background (Fig. 5*b*). It is clear that after a 5-min pulse essentially no radiolabeled *tatC* gene product can be visualized (Fig. 5*b*). In contrast, the radiolabeled polypeptides corresponding to the *tatA* and *tatD* gene products remain stable even after a 60-min chase (Fig. 5*b*). Thus the *tatC* gene product appears to be rapidly degraded in the absence of an active *tatB* gene.

In order to eliminate any possibility that the Δ*tatB* allele had a polar effect on the transcription or translation of the downstream *tatC* gene an *in vivo* expression study was undertaken. A translational *tatC*::*lacZ* fusion was constructed using a "gene-replacement" strategy as described under "Experimental Procedures" in which the *tatC* gene was replaced between codons 3 and 255 by a complete in-frame *lacZ* gene (minus stop codon) encoding β-galactosidase. The *tatC*::*lacZ* fusion was placed downstream of the native *tat* promoter and the intact *tatA* and *tatB* genes on plasmid pFAT23Z, and also on a similar plasmid harboring the Δ*tatB* allele present on the chromosome of BØD, pFAT24Z. When expressed in multicopy in aerobically grown MC4100 (Tat$^+$), values of 480 and 330 Miller units of β-galactosidase activity were recorded for pFAT23Z and pFAT24Z, respectively (compared with a basal level of 1 unit in the strains without the *tatC*::*lacZ* fusion). When *tatC* translation was measured in a Tat$^-$ strain (DADE) similar values were obtained (data not shown). These data strongly suggest that transcription and translation of *tatC* would not be significantly impaired by the presence of the upstream Δ*tatB* allele.

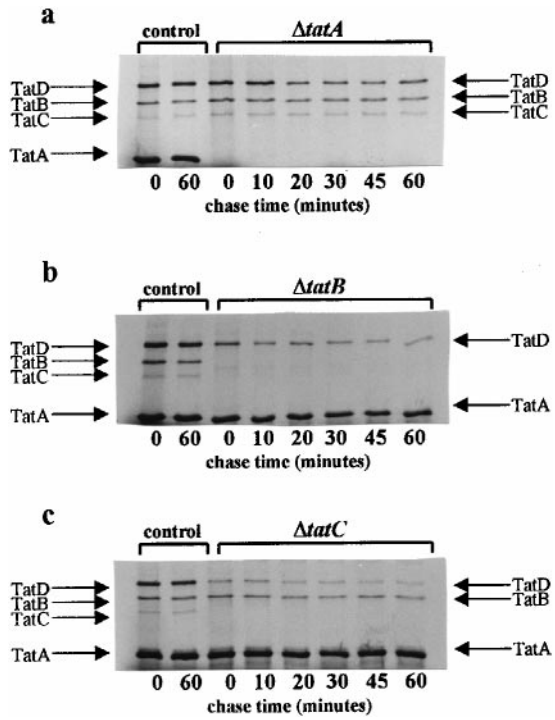

FIG. 5. **The *tatC* gene product is destabilized in the absence of an active *tatB* gene.** Pulse-chase analysis of *tat* gene products expressed in DADE (Δ*tatABCD*, Δ*tatE*) were performed as described under "Experimental Procedures." After a 5-min pulse with [^{35}S]methionine the cells were chased with non-radioactive methionine for a total of 60 min. Whole cell aliquots were taken at the time points indicated and reactions stopped by flash-freezing in liquid nitrogen. Proteins were separated by SDS-PAGE (12.5% (w/v)), and exposed to photographic film overnight. "Control" samples in each experiment were a pulse labeling of the products of the *tatABCD* operon harbored on pFAT65. *a,* pulse labeling of the products of *tat*(Δ*A*)*BCD* (pFAT222). *b,* pulse labeling of the products of *tatA*(Δ*B*)*CD* (pFAT217). *c,* pulse labeling of the products of *tatAB*(Δ*C*)*D* (pFAT228).

We are therefore confident that the TatC$^-$ phenotype displayed in a *tatB*-null background (Fig. 5*b*) is not a consequence of transcriptional or translational polarity of the *tatB* deletion on *tatC*. Furthermore, a second downstream gene, *tatD*, is still transcribed and translated in these experiments, and what is more, the identical chromosomal Δ*tatB* mutation can be complemented by *tatB* alone, thus demonstrating that the essential TatC protein must be synthesized in this strain (Table IV).

A similar experiment using pFAT65 mutagenized with the Δ*tatC* allele present on the chromosome of B1LK0 (10), shows that the remaining *tat* operon products are synthesized and remain stable even after a 60-min chase with non-radioactive methionine (Fig. 5*c*). Thus, while TatB is required for TatC stability the converse does not seem to apply. Finally, introduction of the Δ*tatA* allele present on the chromosome of strain JARV16 into pFAT65 does not affect the stability of the remaining *tat* operon products (Fig. 5*a*). Note also that none of the strains tested in these pulse-chase experiments has an intact *tatE* gene, thus TatE has no significant effect on the stability of the other Tat proteins.

Taken together, these results suggest that TatB, but not the other Hcf106 homologues TatA and TatE, has a function in stabilizing TatC, possibly because the two proteins form a

[4] M. Wexler, F. Sargent, R. L. Jack, N. R. Stanley, E. G. Bogsch, C. Robinson, B. C. Berks, and T. Palmer, submitted for publication.

complex. In the context of this hypothesis, it is likely that TatB forms a scaffold onto which TatC assembles. Also, we suggest that the deleterious effect of overproducing the TatB protein could be explained if the TatA/E and TatC proteins interact only when bound to a central TatB polypeptide. In this case, such an increase in TatB levels would make it unlikely that the other Tat proteins are bound to the same TatB molecule with a concomitant reduction in translocase activity. While we suspect that the TatB protein itself has a vital role in Tat-dependent transport, it is not advisable at this stage to exclude the possibility that the phenotype of a *tatB* null allele may be mediated entirely by the effect of this mutation on the stability of the TatC protein. However, it has not proven possible to demonstrate any suppression of the Δ*tatB* strain mutant phenotype by increasing the levels of *tatC* transcript via a high copy number plasmid bearing only *tatC* (data not shown).

Distinct "TatA-like" and "TatB-like" Proteins on the Tat Protein Export Pathway?—At least two genes coding for proteins of the Hcf106 family are coded in the complete genomes of all prokaryotes possessing the Tat system, with the exception of *Rickettsia prowazekii* which appears to encode but a single such protein. The bipartite division of function between Hcf106-like proteins found in *E. coli* is thus likely to be a general feature of Tat systems. We have tested this idea by heterologous complementation experiments using *H. pylori* 26695 Hcf106 homologues. In *H. pylori*, genes for two such proteins, *HP0320* and *HP1060*, are found at separate chromosomal loci, with *HP1060* apparently co-transcribed with a gene, *HP1061*, encoding a putative TatC homologue (26). The *HP0320* and *HP1060* genes, together with their putative promoter regions, were independently cloned into pBluescript and tested for their ability to restore the *E. coli* Δ*tatA*Δ*tatE, pcnB1* (JARV16-P) or Δ*tatB, pcnB1* (BØD-P) strains to a TorA$^+$ phenotype. The *HP0320* gene was found to complement the Δ*tatA*Δ*tatE,* but not the Δ*tatB* strain (Table IV), strongly suggesting that the *HP0320* gene product is functionally "TatA-like" and further supporting our proposal that there are two classes of Hcf106 homologues with distinct roles in Tat systems.

Primary sequence analysis would appear to predict that the *HP1060* gene should encode a polypeptide more closely related to *E. coli* TatB rather than TatA/E. However, in contrast to the results presented for the *HP0320* gene, *HP1060* was unable to complement either *E. coli* mutant (Table IV). Thus if *HP1060* does indeed code for a TatB-like protein, then the sequence constraints placed on such proteins are apparently more stringent than those for the TatA type.

In the present study we suggest that there are two functionally distinct classes of Hcf106-like proteins: "TatA class" and "TatB class." The exact roles of these two classes in Tat-dependent transport are unclear, but we have been unable to obtain any evidence that would support the idea that the two classes of Hcf106-like proteins interact with different sets of substrate molecules. Our data suggest that TatB class proteins may form a specific complex with TatC proteins, and that the sequence constraints on the TatA class proteins are considerably more relaxed than those on the TatB class. Therefore is it possible, using the large amount of sequence data available for putative Hcf106 homologues encoded by bacterial genomes, to define amino acid sequence features that can distinguish the two functional classes?

Such features can indeed be identified for the obviously TatA class and TatB class proteins from *E. coli* and other Proteobacteria (for example *Hemophilus influenzae*, *Azotobacter chroococcum*, and *H. pylori*) in which the gene encoding the TatB class protein is directly linked to, and probably co-transcribed with, the gene coding for TatC. In these organisms, only the TatB class proteins have the essential proline residue (Pro^{22} in *E. coli* TatB) identified by Weiner *et al*. (9). This residue, together with an invariant preceding glycine residue (Gly^{21} in *E. coli* TatB), may well form a flexible hinge region between the predicted N-terminal transmembrane helix and the following predicted amphipathic helix. Interestingly, the bacterial TatA class proteins also harbor this invariant glycine residue (Gly^{21} in *E. coli* TatA and Gly^{21} in *E. coli* TatE). In the case of TatA class proteins, however, this glycine is not followed by a proline but instead preceded by a conserved phenylalanine residue (Phe^{20} in *E. coli* TatA) and then followed by a second conserved phenylalanine in the predicted amphipathic helix (Phe^{39} of *E. coli* TatA). Neither phenylalanine residue is conserved in the TatB class protein sequences. Most intriguingly, the predicted N-terminal transmembrane helix of TatB class proteins contains a conserved charged residue, Glu^{8} of *E. coli* TatB, which we speculate may be involved, for example, in proton gating during the translocation event or perhaps in maintaining a strong salt-bridge interaction with TatC. Finally, the C-terminal domain of TatB class proteins would appear to be far longer than that of TatA class proteins and encompasses a greatly extended amphipathic region with a string of glutamic acid residues on the polar face. Clearly extensive site-directed mutagenic studies will be required to define further the biological roles of TatA class and TatB class proteins.

In conclusion, however, we concede that none of the above criteria is consistently able to divide the multiple Hcf106 family proteins of each non-Proteobacterial organism into two separate classes. It is therefore conceivable that more than one type of sequence, or combination of sequences, can be used to form each of the two Hcf106 structures required for the operation of the Tat apparatus.

Acknowledgments—We thank Dr. Gary Sawers for valuable discussions and advice, and critical reading of the manuscript. We are also grateful to Dr. Long-Fei Wu for comments on the data presented in this work and for providing strain MCMTA. We acknowledge Prof. David H. Boxer for providing antisera to formate dehydrogenase-N and to hydrogenase-2 and we thank Dr. Erik H. Manting for the cold mild osmotic shock protocol for recovery of periplasmic proteins. Finally, we acknowledge Dr. Kim Hardie, Dr. Nicky Hughes, and Dr. Dave Kelly for the kind gifts of *H. pylori* chromosomal DNA.

REFERENCES

1. Pugsley, A. G. (1993) *Microbiol. Rev.* **57,** 50–108
2. Danese, P. N., and Silhavy, T. J. (1998) *Annu. Rev. Genet.* **32,** 59–94
3. von Heijne, G. (1985) *J. Biol. Chem.* **184,** 99–105
4. Santini, C-L., Ize, B., Chanal, A., Müller, M., Giordano, G., and Wu, L-F. (1998) *EMBO J.* **17,** 101–112
5. Cristóbal, S., de Gier, J-W., Nielsen, H., and von Heijne, G. (1999) *EMBO J.* **18,** 2982–2990
6. Berks, B. C. (1996) *Mol. Microbiol.* **22,** 393–404
7. Settles, A. M., and Martienssen, R. (1998) *Trends Cell Biol.* **8,** 494–501
8. Dalbey, R. E., and Robinson, C. (1999) *Trends Biochem. Sci.* **24,** 17–22
9. Weiner, J. H., Bilous, P. T., Shaw, G. M., Lubitz, S. P., Frost, L., Thomas, G. H., Cole, J. A., and Turner, R. J. (1998) *Cell* **93,** 93–101
10. Bogsch, E. G., Sargent, F., Stanley, N. R., Berks, B. C., Robinson, C., and Palmer, T. (1998) *J. Biol. Chem.* **273,** 18003–18006
11. Settles, A. M., Yonetani, A., Baron, A., Bush, D. R., Cline, K., and Martienssen, R. (1997) *Science* **278,** 1467–1470
12. Sargent, F., Bogsch, E. G., Stanley, N. R., Wexler, M., Robinson, C., Berks, B. C., and Palmer, T. (1998) *EMBO J.* **17,** 3640–3650
13. Chanal, A., Santini, C-L., and Wu, L-F. (1998) *Mol. Microbiol.* **30,** 673–676
14. Casadaban, M. J., and Cohen, S. N. (1979) *Proc. Natl. Acad. Sci. U. S. A.* **76,** 4530–4533
15. Sauter, M., Böhm, R., and Böck, A. (1992) *Mol. Microbiol.* **6,** 1523–1532
16. Tabor, S., and Richardson, C. C. (1985) *Proc. Natl. Acad. Sci. U. S. A.* **82,** 1074–1078
17. Sambrook, J., Fritsch, E. F., and Maniatis, T. (1989) *Molecular Cloning: A Laboratory Manual,* 2nd Ed., Cold Spring Harbor Laboratory Press, Cold Spring Harbor, NY
18. Cohen, G. N., and Rickenberg, H. W. (1956) *Ann. Inst. Pasteur* (*Paris*) **91,** 693–720
19. Sawers, R. G., Ballantine, S. P., and Boxer, D. H. (1985) *J. Bacteriol.* **164,** 1324–1331
20. Hamilton, C. M., Aldea, M., Washburn, B. K., Babitzke, P., and Kushner, S. R. (1989) *J. Bacteriol.* **171,** 4617–4622

21. Menon, N. K., Robbins, J., Peck, H. D., Jr., Chatelus, C. Y., Choi, E.-S., and Przybyla, A. E. (1990) *J. Bacteriol.* **172,** 1969–1977
22. Menon, N. K., Chatelus, C. Y., Dervartanian, M., Wendt, J. C., Shanmugam, K. T., Peck, H. D., Jr., and Przybyla, A. E. (1994) *J. Bacteriol.* **176,** 4416–4423
23. Miller, J. H. (1992) *A Short Course in Bacterial Genetics*, Cold Spring Harbor Laboratory Press, Cold Spring Harbor, NY
24. Bartolomé, B., Jubete, Y., Martínez, E., and de la Cruz, F. (1991) *Gene* (*Amst.*) **102,** 75–78
25. Jayaraman, P.-S., Peakman, T., Busby, S., Quincey, R., and Cole, J. A. (1987) *J. Mol. Biol.* **196,** 281–788
26. Tomb, J.-F., *et al*. (1997) *Nature* **388,** 539–547
27. Osborn, M. J., Gander, J. E., and Parisi, E. (1972) *J. Biol. Chem*. **247,** 3973–3986
28. Ballantine, S. P., and Boxer, D. H. (1985) *J. Bacteriol.* **163,** 454–459
29. Graham, A., Jenkins, H. E., Smith, N. H., Mandrand-Berthelot, M.-A., Haddock, B. A., and Boxer, D. H. (1980) *FEMS Microbiol. Lett.* **7,** 145–151
30. Rodrigue, A., Boxer, D. H., Mandrand-Berthelot, M. A., and Wu, L.-F. (1996) *FEBS Lett.* **392,** 81–86
31. Sargent, F., Ballantine, S. P., Rugman, P. A., Palmer, T., and Boxer, D. H. (1998) *Eur. J. Biochem.* **255,** 746–754
32. Lowry, O. H., Rosebrough, N. J., Farr, A. L., and Randall, R. J. (1951) *J. Biol. Chem.* **193,** 265–275
33. Bilous, P. T., and Weiner, J. H. (1985) *J. Bacteriol.* **162,** 1151–1155
34. Silvestro, A., Pommier, J., and Giordano, G. (1988) *Biochim. Biophys. Acta* **954,** 1–13
35. Atlung, T., Nielson, A., and Hansen, F. G. (1989) *J. Bacteriol.* **171,** 1683–1691
36. Méjean, V., Iobbi-Nivol, C., Lepelletier, M., Giordano, G., Chippaux, M., and Pascal, M. C. (1994) *Mol. Microbiol*. **11,** 1169–1179
37. Bilous, P. T., Cole, S. T., Anderson, W. F., and Weiner, J. H. (1988) *Mol. Microbiol.* **2,** 785–795
38. Berg, B. L., Li, J., Heider, J., and Stewart, V. (1991) *J. Biol. Chem.* **266,** 22380–22385
39. Bernhard, M., Schwartz, E., Rietdorf, J., and Friedrich, B. (1996) *J. Bacteriol.* **178,** 4522–4529
40. Rodrigue, A., Chanal, A., Beck, K., Müller, M., and Wu, L-F. (1999) *J. Biol. Chem.* **274,** 13223–13228
41. Sawers, G. (1994) *Antonie van Leeuwenhoek* **66,** 57–88
42. Wanner, B. L. (1996) in *Escherichia coli and Salmonella: Cellular and Molecular Biology* (Neidhardt, F. C., ed) 2nd Ed., ASM Press, Washington, D. C.
43. Ballantine, S. P., and Boxer, D. H. (1986) *Eur. J. Biochem.* **156,** 277–284
44. Wu, L-F., and Mandrand, M-A. (1993) *FEMS Microbiol. Rev.* **104,** 243–269
45. von Heijne, G. (1986) *EMBO J.* **5,** 3021–3027
46. Bernhard, M., Benelli, B., Hochkoeppler, A., Zannoni, D., and Friedrich, B. (1997) *Eur. J. Biochem.* **248,** 179–186
47. Gross, R., Simon, J., Theis, F., and Kröger, A. (1998) *Arch. Microbiol.* **170,** 50–58
48. Liu, J. D., and Parkinson, J. S. (1989) *J. Bacteriol.* **171,** 1254–1261

Sec-independent Protein Translocation in *Escherichia coli* : A DISTINCT AND PIVOTAL ROLE FOR THE TatB PROTEIN

Frank Sargent, Nicola R. Stanley, Ben C. Berks and Tracy Palmer

J. Biol. Chem. 1999, 274:36073-36082.
doi: 10.1074/jbc.274.51.36073